DALTON
FULL PAPER

Cadmium(II), bismuth(III), lead(II) and thallium(I) crown thioether chemistry: synthesis and crystal structures of $[(CdI_2)_2([24]aneS_8)]$, $[(BiCl_3)_2([24]aneS_8)]$, $[Pb_2([28]aneS_8)][ClO_4]_4$ and $[Tl([24]aneS_8)]PF_6$ ($[24]aneS_8$ = 1,4,7,10,13,16,19,22-octathiacyclotetracosane; $[28]aneS_8$ = 1,4,8,11,15,18,22,25-octathiacyclooctacosane)

Alexander J. Blake,[a] Dieter Fenske,[b] Wan-Sheung Li,[a] Vito Lippolis[a] and Martin Schröder*[a]

[a] *School of Chemistry, The University of Nottingham, Nottingham, UK NG7 2RD*
[b] *Institüt für Anorganische Chemie, Universität Karlsruhe, Engesserstrasse, Gebäude-NR. 30.45, D-76128 Karlsruhe, Germany*

Received 3rd July 1998, Accepted 7th September 1998

The complexes $[(CdI_2)_2([24]aneS_8)]$, $[(BiCl_3)_2([24]aneS_8)]$, $[Pb_2([28]aneS_8)][ClO_4]_4$ and $[Tl([24]aneS_8)]PF_6$ ($[24]aneS_8$ = 1,4,7,10,13,16,19,22-octathiacyclotetracosane, $[28]aneS_8$ = 1,4,8,11,15,18,22,25-octathiacyclooctacosane) have been prepared, characterized and their crystal structures determined. In $[(CdI_2)_2([24]aneS_8)]$ two CdI_2 units are bound to the macrocycle forming a discrete centrosymmetric binuclear complex, Cd(1)–I(1) 2.7551(11), Cd(1)–I(2) 2.6944(8), Cd(1)–S(1) 2.817(2), Cd(1)–S(4) 2.615(2), Cd(1)–S(7) 2.927(2) Å. In $[(BiCl_3)_2([24]aneS_8)]$ two $BiCl_3$ units are weakly bonded to the thioether crown, Bi–S 3.134(2)–3.313(2) Å, to give a discrete centrosymmetric binuclear complex with the two metal centres disposed on opposite sides of the mean plane of the macrocycle. In $[Pb_2([28]aneS_8)][ClO_4]_4$ an S_4O_4 co-ordination is realized at each Pb^{II} sitting in the macrocyclic cavity. The two Pb^{II} are bridged by two ClO_4^- ions, Pb–S 2.861(2)–2.998(2), Pb–O 2.701(7)–2.936(6) Å. In contrast, $[Tl([24]aneS_8)]PF_6$ adopts a polymeric structure in which each Tl^I bridges two thioether crowns to give an infinite sinusoidal chain. The $[S_4 + S_4]$ co-ordination sphere at the metal centre is satisfied by two half ligands in a sandwich arrangement, Tl–S 3.2413(11)–3.4734(14) Å.

Introduction

The co-ordination chemistry of crown thioethers has been the subject of great interest over the past decade.[1] These macrocycles can form stable, inert complexes with a wide range of transition metal ions,[2–12] sometimes forcing the metal centre to adopt unusual co-ordination geometries and/or oxidation states.[1,13–15] The majority of these studies have focused on the co-ordination chemistry of 1,4,7-trithiacyclononane ($[9]aneS_3$), 1,4,7,10-tetrathiacyclododecane ($[12]aneS_4$), 1,5,9,13-tetrathiacyclohexadecane ($[16]aneS_4$) and 1,4,7,10,13,16-hexathiacyclooctadecane ($[18]aneS_6$) in order to understand the relationships between the stereochemical and redox characteristics of the corresponding transition metal complexes. In contrast, the co-ordination chemistry of larger rings such as 1,4,7,10,13,16,19,22-octathiacyclotetracosane ($[24]aneS_8$) and 1,4,8,11,15,18,22,25-octathiacyclooctacosane ($[28]aneS_8$) is less well studied[3,16,17] and the examination of p-block metals ions and d^{10} transition metal ions still remains an open area of investigation. Few examples of thioether macrocyclic complexes of Cd^{II}, Hg^{II} and Au^I have been reported[15,18–21] and it is only recently that the corresponding co-ordination chemistry of Ag^I has received any attention.[1,22–29] Furthermore, the only examples of structurally characterized complexes of p-block elements with thioether crowns are limited to $[Pb([9]aneS_3)_2(OClO_3)_2]$,[30] $[AlMe_3([12]aneS_4)]$,[31] $[AlMe_3([14]aneS_4)]$,[32] $[Tl([9]aneS_3)]PF_6$,[33] $[Tl([18]aneS_6)]PF_6$,[34] $[BiCl_3([12]aneS_4)]$,[35] $[BiCl_3([15]aneS_5)]\cdot 0.5MeCN$,[35] $[SbCl_3([9]aneS_3)]$,[36] $[(SbCl_3)_2([18]aneS_6)]$,[36] $[(SnCl_3)_3([9]aneS_3)_2]$[37] and $[(SnCl_4)_2([18]aneS_6)]\cdot MeCN$.[37]

Considering that macrocyclic polythioethers also represent a useful starting point for designing selective metal complexation agents for the uptake and transportation of toxic heavy-metal ions, we have recently reported the synthesis, crystal structures and electrochemical properties of complexes of Ag^I, Hg^{II} and Au^I with $[24]aneS_8$ and $[28]aneS_8$.[16] As an extension of this investigation, we report herein the synthesis and crystal structures of $[(CdI_2)_2([24]aneS_8)]$, $[(BiCl_3)_2([24]aneS_8)]$, $[Pb_2([28]aneS_8)][ClO_4]_4$ and $[Tl([24]aneS_8)]PF_6$. With the exception of our work on $[Cu_2([24]aneS_8)][BF_4]_2$, $[Cu_2([28]aneS_8)][ClO_4]_2$[3] and on related complexes of Ag^I, Hg^{II} and Au^I,[16] these represent the only examples of complexes of these large-ring crown thioethers to have been structurally characterized.

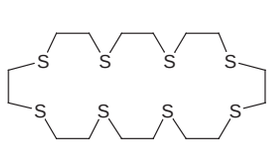

$[24]aneS_8$

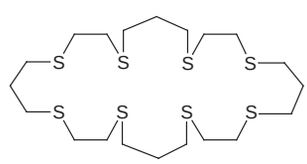

$[28]aneS_8$

Results and discussion

$[(CdI_2)_2([24]aneS_8)]$

Reaction of $[24]aneS_8$ with 2 equivalents of CdI_2 in MeCN–CH_2Cl_2 (1:1 v/v) affords a white precipitate after stirring at room temperature for 1 h. Analytical and mass spectrometric data supported the stoichiometry $[(CdI_2)_2([24]aneS_8)]$ and colourless block-shaped crystals suitable for X-ray diffraction studies were obtained by diffusion of Et_2O vapour into a solution of the complex in $MeNO_2$–thf (1:1 v/v).

A single crystal structure analysis confirms the complex to be the binuclear species $[(CdI_2)_2([24]aneS_8)]$ (Fig. 1, Table 1). As in $[(HgBr_2)_2([24]aneS_8)]$,[16b] the complex lies across a crystallographic inversion centre with the asymmetric unit consisting of one CdI_2 moiety and half of a $[24]aneS_8$ macrocycle. Each Cd^{II} has an overall distorted trigonal bipyramidal geometry, being co-ordinated by three consecutive S atoms of the macrocycle

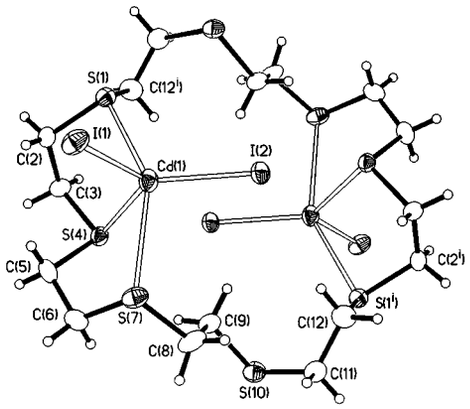

Fig. 1 View of $[(CdI_2)_2([24]aneS_8)]$ with numbering scheme adopted; i $-x$, $-y+1$, $-z$. Displacement ellipsoids are drawn at 50% probability.

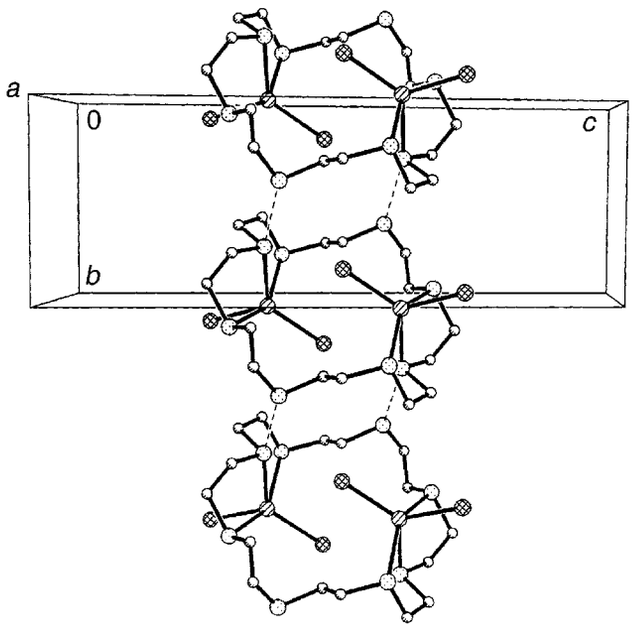

Fig. 2 Packing diagram for $[(CdI_2)_2([24]aneS_8)]$ viewed along the *a* axis.

and two I^- ligands, Cd(1)–I(1) 2.7551(11), Cd(1)–I(2) 2.6944(8), Cd(1)–S(1) 2.817(2), Cd(1)–S(4) 2.615(2), Cd(1)–S(7) 2.927(2) Å. The two apical Cd–S bond distances to S(1) and S(7) [S(1)–Cd(1)–S(7) 147.39(5)°] are much longer than the bond to S(4) and, as for $[(HgBr_2)_2([24]aneS_8)]$,[16b] this could be a consequence of the different dispositions of the three co-ordinated S donors relative to the cavity of the macrocycle, S(4) being *endo*- and S(1) and S(7) being *exo*-oriented. However, even though the two Hg–S_{ap} interactions in $[(HgBr_2)_2([24]aneS_8)]$[16b] differ considerably, Hg–S_{ap} 2.836(4), 3.110(4) Å, the average Hg–S bond distances, 2.8(1) Å, is practically identical to the average of the Cd–S bonds in $[(CdI_2)_2([24]aneS_8)]$, 2.79(8) Å. This underlines the similarity of the co-ordination geometry imposed by $[24]aneS_8$ at CdI_2 and HgI_2 moieties. [In this paper, the estimated standard deviations (σ) on each mean M–S distance were calculated using the expression $\sigma^2(x) = \Sigma_{i=1}^{n}(x_i - \bar{x})^2/n(n-1)$ where n is the number of data averaged and $\bar{x}$ is their mean.] The Cd···Cd distance across the inversion centre is 5.797(2) Å with the two CdI_2 moieties disposed on opposite sides of the macrocyclic ring, to give an overall *anti* configuration. Selected bond lengths and angles are summarized in Table 1. The crystal lattice comprises stacks of the binuclear complex propagating along the *b* axis *via* S···S contacts of 3.636(2) Å between successive units (Fig. 2). Interestingly, as for $[(HgBr_2)_2([24]aneS_8)]$,[16b] the S atoms involved in these long range S···S contacts are the one not involved in any co-ordination [S(10)] and the one which shows the shortest Cd–S bond distance [S(4)].

To our knowledge only four cadmium(II) complexes of thioether crowns have been reported, namely $[Cd([15]aneS_5)][ClO_4]_2\cdot H_2O$,[21] $[Cd([16]aneS_4)][ClO_4]_2$,[20a] $[Cd([9]aneS_3)_2][BF_4]_2\cdot 2MeNO_2$[20b] and $[CdI_2([9]aneS_3)]_2$.[20c] These complexes have five, four, six and three S-donors bound to the metal centre, respectively, with mean Cd–S bond distances of 2.76(2), 2.618(1), 2.654(2) and 2.767(7) Å. Comparing these data with a value of 2.79(8) Å for the mean Cd–S distance in $[(CdI_2)_2([24]aneS_8)]$ where three S-donors bind to Cd^{II}, it is now apparent that the proposed direct correlation[21] between the metal–sulfur bond lengths and the number of co-ordinated S atoms has not been conclusively established. When the estimated standard deviations on the mean distances are taken into account, the mean metal–sulfur bonds do not change significantly as the number of co-ordinated S-donors increases. Also, in mercury(II) complexes of thioether crowns for which this relationship was first proposed,[20a] the average Hg–S bond distances do not differ significantly between $[Hg([16]aneS_4)][ClO_4]_2$,[20a] $[Hg([14]aneS_4)(OH_2)][ClO_4]_2$,[18] $[(HgCl_2)([14]aneS_4)]$[18] (four co-ordinated S-donors) and $[Hg([15]aneS_5)][PF_6]_2$[19] (five co-ordinated S-donors) [Hg–S_{av} 2.597(5), 2.61(4), 2.64(3) and 2.59(5) Å, respectively] and $[Hg([9]aneS_3)_2][PF_6]_2$[15a] [six co-ordinated S-donors, Hg–S_{av} 2.69(2) Å]. For $[(HgBr_2)_2([24]aneS_8)]$,[16b] Hg–S_{av} 2.8(1) Å for three Hg–S distances, and 2.71(8) Å if the Hg–S_{ap} long interaction of 3.110(4) Å is excluded from the calculation of the mean on the grounds that it is quite beyond the value of 2.8 Å which is the sum of the formal ionic radii for Hg^{II} (0.96 Å) and S (1.84 Å).[38]

Table 1 Selected bond lengths (Å), angles (°) and torsion angles (°) with standard uncertainties for $[(CdI_2)_2([24]aneS_8)]$

Cd(1)–S(1)	2.817(2)	Cd(1)–I(1)	2.7551(11)
Cd(1)–S(4)	2.615(2)	Cd(1)–I(2)	2.6944(8)
Cd(1)–S(7)	2.927(2)		
S(1)–Cd(1)–S(4)	80.22(5)	S(4)–Cd(1)–I(1)	113.26(4)
S(1)–Cd(1)–S(7)	147.39(5)	S(4)–Cd(1)–I(2)	126.04(4)
S(1)–Cd(1)–I(1)	86.73(4)	S(7)–Cd(1)–I(1)	88.16(4)
S(1)–Cd(1)–I(2)	112.67(4)	S(7)–Cd(1)–I(2)	97.84(4)
S(4)–Cd(1)–S(7)	72.36(5)	I(1)–Cd(1)–I(2)	119.42(3)

C(12^{i})–S(1)–C(2)–C(3)	60.7(5)
S(1)–C(2)–C(3)–S(4)	61.5(6)
C(2)–C(3)–S(4)–C(5)	81.7(5)
C(3)–S(4)–C(5)–C(6)	177.9(4)
S(4)–C(5)–C(6)–S(7)	58.3(6)
C(5)–C(6)–S(7)–C(8)	−126.7(5)
C(6)–S(7)–C(8)–C(9)	70.4(6)
S(7)–C(8)–C(9)–S(10)	−171.3(4)
C(8)–C(9)–S(10)–C(11)	−62.8(5)
C(9)–S(10)–C(11)–C(12)	−64.3(5)
S(10)–C(11)–C(12)–S(1^{i})	−57.7(6)
C(11)–C(12)–S(1^{i})–C(2^{i})	−150.0(4)

Symmetry transformation used to generate equivalent atoms i $-x$, $-y+1$, $-z$.

Presumably, steric factors associated with the preferred co-ordination geometry of the thioether macrocyclic ligands together with the nature of co-ligands will have a marked influence on the observed M−S bond lengths especially when soft and polarizable metal ions such as Cd^{II} and Hg^{II} and thioether donors are considered. It may therefore be very difficult to make generalizations about potential trends in observed M–S bond distances in these systems.

$[(BiCl_3)_2([24]aneS_8)]$

Reaction of $[24]aneS_8$ with 2 molar equivalents of $BiCl_3$ in MeCN affords a white precipitate after stirring for 2 h at room temperature under N_2. On the basis of microanalytical

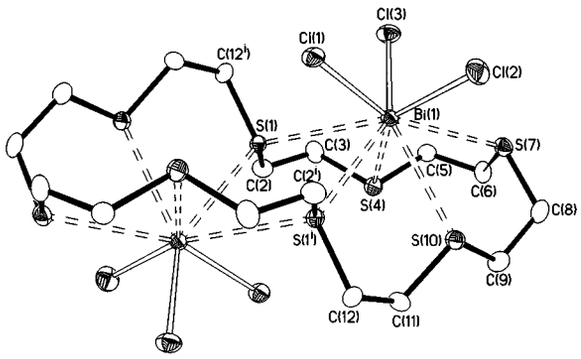

Fig. 3 View of $[(BiCl_3)_2([24]aneS_8)]$ with numbering scheme adopted; i $-x$, $-y$, $-z$. Displacement ellipsoids are drawn at 50% probability, hydrogen atoms have been omitted for clarity.

Table 2 Selected bond lengths (Å), angles (°) and torsion angles (°) with standard uncertainties for $[(BiCl_3)_2([24]aneS_8)]$

Bi(1)–Cl(1)	2.598(2)	Bi(1)–S(4)	3.209(2)
Bi(1)–Cl(2)	2.522(2)	Bi(1)–S(7)	3.134(2)
Bi(1)–Cl(3)	2.566(2)	Bi(1)–S(10)	3.144(2)
Bi(1)–S(1)	3.227(2)	Bi(1)–S(1^i)	3.313(2)
Cl(1)–Bi(1)–Cl(2)	86.29(6)	Cl(3)–Bi(1)–S(10)	147.71(5)
Cl(1)–Bi(1)–Cl(3)	89.79(6)	Cl(1)–Bi(1)–S(1^i)	69.69(5)
Cl(2)–Bi(1)–Cl(3)	93.60(6)	Cl(2)–Bi(1)–S(1^i)	104.93(6)
Cl(1)–Bi(1)–S(1)	70.95(5)	Cl(3)–Bi(1)–S(1^i)	150.94(5)
Cl(2)–Bi(1)–S(1)	157.23(5)	S(1)–Bi(1)–S(4)	63.28(4)
Cl(3)–Bi(1)–S(1)	87.11(5)	S(1)–Bi(1)–S(7)	127.93(4)
Cl(1)–Bi(1)–S(4)	133.65(5)	S(1)–Bi(1)–S(10)	110.88(5)
Cl(2)–Bi(1)–S(4)	139.35(5)	S(4)–Bi(1)–S(7)	64.78(5)
Cl(3)–Bi(1)–S(4)	81.27(5)	S(4)–Bi(1)–S(10)	83.42(5)
Cl(1)–Bi(1)–S(7)	158.40(5)	S(7)–Bi(1)–S(10)	66.03(5)
Cl(2)–Bi(1)–S(7)	74.54(6)	S(1)–Bi(1)–S(1^i)	67.18(5)
Cl(3)–Bi(1)–S(7)	81.72(6)	S(4)–Bi(1)–S(1^i)	97.86(4)
Cl(1)–Bi(1)–S(10)	120.93(5)	S(7)–Bi(1)–S(1^i)	124.42(4)
Cl(2)–Bi(1)–S(10)	79.92(6)	S(10)–Bi(1)–S(1^i)	59.50(4)

C(12^i)–S(1)–C(2)–C(3)	90.2(5)
S(1)–C(2)–C(3)–S(4)	65.6(6)
C(2)–C(3)–S(4)–C(5)	−173.5(5)
C(3)–S(4)–C(5)–C(6)	174.7(5)
S(4)–C(5)–C(6)–S(7)	−68.1(5)
C(5)–C(6)–S(7)–C(8)	139.3(5)
C(6)–S(7)–C(8)–C(9)	−75.6(5)
S(7)–C(8)–C(9)–S(10)	−67.0(6)
C(8)–C(9)–S(10)–C(11)	169.6(5)
C(9)–S(10)–C(11)–C(12)	177.5(5)
S(10)–C(11)–C(12)–S(1^i)	54.7(6)
C(11)–C(12)–S(1^i)–C(2^i)	−136.2(5)

Symmetry transformation used to generate equivalent atoms: i $-x$, $-y$, $-z$.

and IR spectroscopic data, the product was assigned as $[(BiCl_3)_2([24]aneS_8)]$. A single crystal structure determination confirms the compound to be a binuclear bismuth(III) complex (Fig. 3, Table 2). Like $[(CdI_2)_2([24]aneS_8)]$, this molecule lies across a crystallographic inversion centre, the macrocycle adopting a sigmoidal conformation generating two symmetry-related cradles over which the two $BiCl_3$ moieties sit. Each Bi^{III} is co-ordinated to five S-donors of the crown and to three Cl^- ligands in a half-sandwich arrangement. Atom S(1) and its symmetry equivalent S(1^i) (i $-x$, $-y$, $-z$) both bridge the two metal centres and this represents the first example of a thioether macrocyclic complex in which S-donors link two metal centres within the same complex cation. The co-ordinated S atoms in the asymmetric unit are not coplanar and the $BiCl_3$ moiety sits centrally over the macrocyclic ring with the Bi atom displaced 1.6003(8) Å from the mean plane defined by S(1), S(4), S(7), S(10) and S(1^i). Three of the Bi–S bond distances, Bi(1)–S(1) 3.227(2), Bi(1)–S(4) 3.209(2), Bi(1)–S(1^i) 3.313(2) Å, are longer than the other two, Bi(1)–S(7) 3.134(2), Bi(1)–S(10) 3.144(2) Å, with an overall mean value of 3.21(3) Å [the sum of the formal ionic radii of S (1.84) and Bi^{III} (1.17) is 3.01 Å].[38] Interestingly, this mean Bi–S distance is similar to that observed for $[BiCl_3([15]aneS_5)]\cdot 0.5MeCN$, 3.17(3) Å,[35] which shows a similar co-ordination sphere at the Bi. In $[BiCl_3([12]aneS_4)]$,[35] which shows four S-donors bound to the $BiCl_3$ unit, the average Bi–S bond distance is 3.07(5) Å. As with other complexes of $BiCl_3$ with thioether crowns, the structural parameters of the $BiCl_3$ unit change very little upon complexation, indicating a relatively weak interaction between the macrocycle and the metal halide; for $[(BiCl_3)_2([24]aneS_8)]$ the mean Bi–Cl bond distance is 2.56(2) Å and the mean Cl–Bi–Cl angle is 90(2)° compared to 2.49 Å(1) and 91(3)° in the parent halide.[39] The crystal lattice features stacks of binuclear units linked along the *b* axis by Cl···Cl and S···S contacts of 3.447(4) and 3.321(3) Å, respectively (Fig. 4). Of interest is the close similarity of the co-ordination geometry around the metal centre in $[(BiCl_3)_2([24]aneS_8)]$ and $BiCl_3$. In the latter the Bi centres is strongly bonded to three chlorine atoms, Bi–Cl 2.468(4)–2.518(7) Å, in a distorted trigonal pyramid with five Cl^- centres located opposite the first three and interacting weakly with the metal ion, Bi···Cl 3.216(9)–3.450(9) Å. The overall eight-fold co-ordination is best described as a trigonal prism with two additional Cl^- donors occupying two of its faces.[39] A similar co-ordination geometry can be envisaged in $[(BiCl_3)_2([24]aneS_8)]$ if we consider that the three Cl^- atoms and S(4), S(10) and S(1^i) form a trigonal prism (the two planes defined by the three Cl^- atoms and the three S atoms are tilted by only 9.4°); S(1) and S(7) then cap the Cl(1)–Cl(3)–S(4)–S(1^i) and Cl(2)–Cl(3)–S(4)–S(10) faces, respectively (Fig. 3).

The crystal structures so far reported suggest that the co-ordination mode of thioether macrocycles to $BiCl_3$ as well as crown ethers[40] depends strongly upon the inflexible character of this metal halide moiety. The macrocyclic ligands therefore have to adopt a conformation which allows between four and six donors to bind to the $BiCl_3$ fragment within the constraints of a half-sandwich structure.

$[Pb_2([24]aneS_8)][ClO_4]_4$ and $[Pb_2([28]aneS_8)][ClO_4]_4$

Treatment of $[24]aneS_8$ with 2 equivalents of $Pb(ClO_4)_2\cdot 3H_2O$ in MeCN–CH_2Cl_2 (1 : 1 v/v) affords a white solid after stirring at room temperature for 2 h. Spectroscopic and microanalytical data suggest the formulation $[Pb_2([24]aneS_8)][ClO_4]_4$. Crystals were grown by diffusion of Et_2O vapour into a solution of the complex in MeCN. Unfortunately, severe crystal twinning prevented a complete elucidation of the crystal structure. In order to obtain information on the binding of very large thioether crowns to Pb^{II}, we repeated the reaction under the same conditions but using $[28]aneS_8$. The IR spectrum of the resulting white solid confirmed the presence of $[28]aneS_8$ and co-ordinated ClO_4^-, while the fast atom bombardment (FAB) mass spectrum in 3-nitrobenzyl alcohol (noba) showed peaks with the correct isotopic distribution for $[^{207}Pb_2([28]aneS_8)(ClO_4)_3]^+$ (M^+, m/z 1250) together with peaks corresponding to successive loss of ClO_4^- counter anions. Elemental analysis confirmed the stoichiometry $[Pb_2([28]aneS_8)][ClO_4]_4$. In order to establish the solid state connectivity and stereochemistry of the product, single crystals were grown by diffusion of Et_2O vapour into a solution of the complex in MeCN. The single crystal structure determination confirms the binuclear nature of the compound (Fig. 5, Table 3). Again, the complex lies across a crystallographic inversion centre with the [28]ane-S_8 crown adopting a flat conformation with all eight S atoms *endo*-oriented, allowing the two Pb^{II} to sit within the ring cavity. An analogous situation has been observed for the complexes $[Ag_2([28]aneS_8)][NO_3]_2$,[16b] $[Au_2([28]aneS_8)][PF_6]_2$[16b] and $[Cu_2([28]aneS_8)][PF_6]_2$[3] in which the two metal centres are also encapsulated within the cavity of the thioether crown. The larger ring size of $[28]aneS_8$ compared to $[24]aneS_8$ is clearly

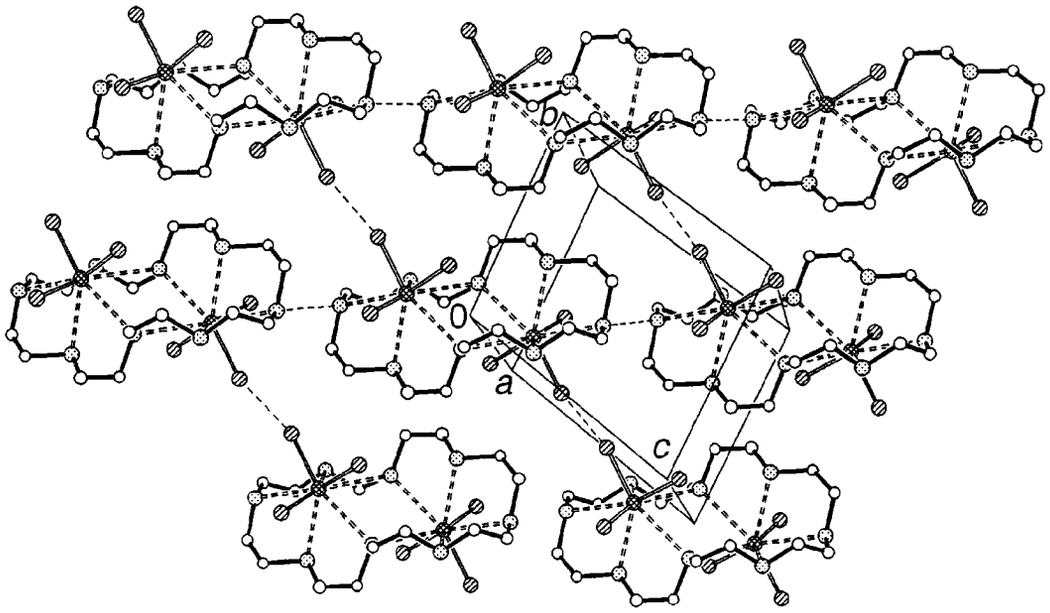

Fig. 4 Packing diagram for $[(BiCl_3)_2([24]aneS_8)]$ viewed approximately along the *a* axis. Single dashed lines indicate the Cl···Cl and S···S contacts.

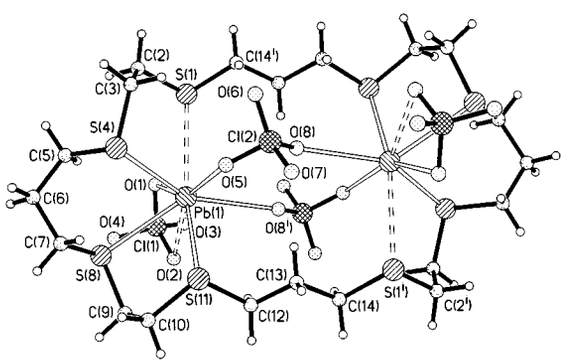

Fig. 5 View of $[Pb_2([28]aneS_8)][ClO_4]_4$ with numbering scheme adopted; i $-x$, $-y$, $-z$. Atoms are not drawn as ellipsoids for clarity reasons and only one component of the disordered O(8) atom is shown.

advantageous for the complexation of large metal ions within the macrocyclic cavity to give discrete binuclear products. Complexes of $[24]aneS_8$ reported so far are either polymeric or binuclear, but with the two metal centres considerably displaced from the mean plane of the ligand. An exception is $[Cu_2([24]aneS_8)][BF_4]_2$[3] but the copper(I) ion is considerably smaller than those discussed herein. In $[Pb_2([28]aneS_8)][ClO_4]_4$ each Pb^{II} is co-ordinated to four S- and four O-donors, two of the latter deriving from a terminal bidentate ClO_4^- ion and two from two ClO_4^- ions bridging the two metal ions within the macrocyclic cavity (Fig. 5). Three of the Pb–S bond distances, Pb(1)–S(4) 2.861(2), Pb(1)–S(8) 2.955(2), Pb(1)–S(11) 2.998(2) Å, are significantly shorter than the fourth, Pb(1)–S(1) 3.137(2) Å. The same trend is observed for the Pb–O bond lengths, Pb(1)–O(1) 2.722(6), Pb(1)–O(5) 2.701(7), Pb(1)–O(8^{i}) 2.795(12), Pb(1)–O(2) 2.936(6) Å, i $-x$, $-y$, $-z$. The only thioether complexes of Pb^{II} previously reported are those with 1,4,7-trithiacyclononane[30] and 1,5-dithiacyclooctan-3-ol;[41] the Pb–S bond distances range from 3.015(5) to 3.208(3) Å and the Pb–O bond lengths to the co-ordinated counter ions (ClO_4^- and NO_3^- respectively) span the range 2.701(10)–2.795(11) Å. Complexes of Pb^{II} with mixed N/S donor macrocyclic ligands[42] also give Pb–S bond distances comparable with that of 3.137(2) Å observed in $[Pb_2([28]aneS_8)][ClO_4]_4$. The only exception is represented by the complex with 1-thia-4,7-diazacyclononane[42*d*] for which the Pb–S distance is 2.860(5) Å. Interestingly, for complexes with these mixed N/S donor macrocyclic ligands, the Pb–O distances of the co-ordinated counter anions are much shorter, ranging from 2.440(14)–2.548(17) Å for the bidentate acetate ion in $[Pb(L^1)(O_2CMe)]PF_6$ (L^1 = 3,13-dithia-6,10-diaza-1,8(2,6)-dipyridinacyclotetradecaphane-6,9-diene)[42*a*] to 2.599(12)–2.761(12) Å for the bidentate ClO_4^- ion in $[Pb(L^2)][ClO_4]_2$ (L^2 = 6,7,8,9,10,11,12,13,19,20-decahydro-5*H*-dibenzo[*e*,*p*][1,4,8,11,14]dithiatriazacycloheptadecane).[42*c*] In $[Pb_2([28]aneS_8)][ClO_4]_4$ the overall

Table 3 Selected bond lengths (Å), angles (°) and torsion angles (°) with standard uncertainties for $[Pb_2([28]aneS_8)][ClO_4]_4$

Pb(1)–S(1)	3.137(2)	Pb(1)–O(1)	2.722(6)
Pb(1)–S(4)	2.861(2)	Pb(1)–O(2)	2.936(6)
Pb(1)–S(8)	2.955(2)	Pb(1)–O(5)	2.701(7)
Pb(1)–S(11)	2.998(2)	Pb(1)–O(8^{i})	2.795(12)
O(5)–Pb(1)–O(1)	152.5(2)	O(5)–Pb(1)–S(1)	84.59(17)
O(5)–Pb(1)–O(8^{i})	82.2(4)	O(5)–Pb(1)–S(4)	67.24(19)
O(5)–Pb(1)–S(11)	68.7(2)	O(5)–Pb(1)–S(8)	122.2(2)
O(5)–Pb(1)–O(2)	155.7(2)	O(1)–Pb(1)–O(8^{i})	97.3(3)
O(1)–Pb(1)–O(2)	48.58(14)	O(1)–Pb(1)–S(1)	67.99(11)
O(1)–Pb(1)–S(4)	104.02(12)	O(1)–Pb(1)–S(8)	76.95(13)
O(1)–Pb(1)–S(11)	138.73(12)	O(8^{i})–Pb(1)–S(1)	93.1(3)
O(8^{i})–Pb(1)–S(4)	146.9(4)	O(8^{i})–Pb(1)–S(8)	135.6(4)
O(8^{i})–Pb(1)–S(11)	87.5(3)	O(8^{i})–Pb(1)–O(2)	82.0(4)
O(2)–Pb(1)–S(1)	114.62(11)	O(2)–Pb(1)–S(4)	131.03(12)
O(2)–Pb(1)–S(8)	61.01(12)	O(2)–Pb(1)–S(11)	92.22(11)
S(1)–Pb(1)–S(4)	72.43(5)	S(1)–Pb(1)–S(8)	123.20(5)
S(1)–Pb(1)–S(11)	152.99(5)	S(4)–Pb(1)–S(8)	74.71(5)
S(4)–Pb(1)–S(11)	92.69(6)	S(8)–Pb(1)–S(11)	71.47(6)

C(14^{i})–S(1)–C(2)–C(3)	−76.7(6)
S(1)–C(2)–C(3)–S(4)	−64.6(7)
C(2)–C(3)–S(4)–C(5)	−54.1(6)
C(3)–S(4)–C(5)–C(6)	−152.8(5)
S(4)–C(5)–C(6)–C(7)	−46.3(8)
C(5)–C(6)–C(7)–S(8)	−51.6(8)
C(6)–C(7)–S(8)–C(9)	−174.3(5)
C(7)–S(8)–C(9)–C(10)	−52.6(7)
S(8)–C(9)–C(10)–S(11)	−57.3(9)
C(9)–C(10)–S(11)–C(12)	−82.8(7)
C(10)–S(11)–C(12)–C(13)	−162.8(5)
S(11)–C(12)–C(13)–C(14)	−176.3(5)
C(12)–C(13)–C(14)–S(1^{i})	−179.4(5)
C(13)–C(14)–S(1^{i})–C(2^{i})	−175.9(5)

Symmetry transformation used to generate equivalent atoms: i $-x$, $-y$, $-z$.

S_4O_4 donation at each Pb^{II} gives a *holodirected*[43] co-ordination geometry around the metal ions with the bonds to the donor atoms evenly distributed about the co-ordination sphere and the $6s^2$ lone pair of Pb^{II} seeming to be stereochemically inactive. Presumably, the separation of the two metal ions within the macrocyclic cavity, Pb···Pb 5.9127(12) Å, allows the ClO_4^- anions to act as bidentate ligands bridging the metal centres by permitting favourable Cl–O–Pb angles. In this way, the inert lone pair of electrons is prevented from expanding the co-ordination sphere of the lead(II) ions.

$[Tl([24]aneS_8)]PF_6$

Treatment of $TlPF_6$ with either 1 or 2 molar equivalents of [24]aneS_8 in $MeCN–CH_2Cl_2$ (1:1 v/v) at room temperature for 3 h affords a colourless solution from which free ligand can be recovered as a white solid after partial removal of the solvent. Colourless block crystals were grown by diffusion of Et_2O vapour into the remaining solution. Infrared spectroscopy and microanalytical data of the product were consistent with the formulation of these crystals as $[Tl([24]aneS_8)]PF_6$. Fast atom bombardment mass spectrometry showed a peak at *m/z* 685 assigned to $[Tl([24]aneS_8)]^+$. A single crystal structure determination was undertaken to define the nature of the interaction between the macrocyclic ligand and the metal ion and this confirmed the complex to be a one-dimensional polymer. Each molecule of [24]aneS_8 lies across a crystallographic inversion centre and is co-ordinated to two thallium(I) ions disposed on opposite sides of the mean plane of the macrocycle in an *anti* configuration. Each Tl^I occupies a two-fold axis and is sandwiched between two symmetry-related halves of two [24]aneS_8 molecules (Fig. 6). Successive $[Tl([24]aneS_8)]^+$ units are related by the *a* glide plane, generating an infinite one-dimensional sinusoidal polymer running along the *a* axis (Fig. 7). An overall [4 + 4] thioether co-ordination at each metal centre results with two Tl–S bond distances, Tl(1)–S(1)

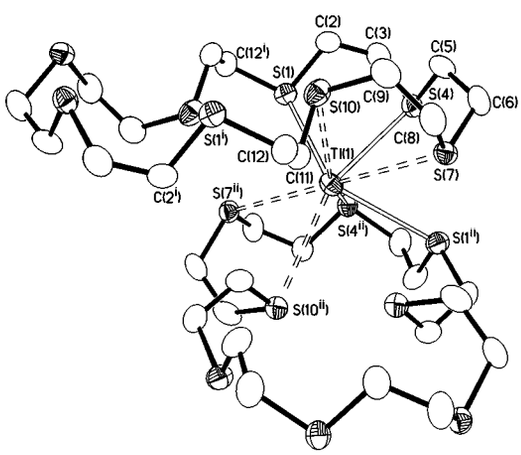

Fig. 6 View of the cation $[Tl([24]aneS_8)]^+$ showing the environment of the Tl^I and the numbering scheme adopted (i $-x + 1, -y + 1, -z + 1$; ii $-x + \frac{1}{2}, y, -z + 1$). Each metal centre is co-ordinated by two half ligands in a sandwich structure. Hydrogen atoms have been omitted for clarity.

Table 4 Selected bond lengths (Å), angles (°) and torsion nangles (°) with standard uncertainties for $[Tl([24]aneS_8)]PF_6$

Tl(1)–S(1)	3.2851(13)	Tl(1)–S(7)	3.4305(14)
Tl(1)–S(4)	3.2413(11)	Tl(1)–S(10)	3.4734(14)
S(1)–Tl(1)–S(4)	63.47(3)	S(1)–Tl(1)–S(7ⁱⁱ)	63.22(3)
S(1)–Tl(1)–S(7)	116.29(3)	S(1)–Tl(1)–S(10ⁱⁱ)	124.48(3)
S(1)–Tl(1)–S(10)	86.24(3)	S(4)–Tl(1)–S(4ⁱⁱ)	69.12(4)
S(4)–Tl(1)–S(7)	62.24(3)	S(4)–Tl(1)–S(7ⁱⁱ)	116.94(3)
S(4)–Tl(1)–S(10)	87.90(3)	S(4)–Tl(1)–S(10ⁱⁱ)	151.66(3)
S(7)–Tl(1)–S(10)	61.34(3)	S(7)–Tl(1)–S(7ⁱⁱ)	179.11(3)
S(1)–Tl(1)–S(1ⁱⁱ)	121.47(4)	S(7)–Tl(1)–S(10ⁱⁱ)	119.18(3)
S(1)–Tl(1)–S(4ⁱⁱ)	68.99(3)	S(10)–Tl(1)–S(10ⁱⁱ)	118.39(4)

C(12ⁱ)–S(1)–C(2)–C(3)	−169.1(3)
S(1)–C(2)–C(3)–S(4)	−66.2(5)
C(2)–C(3)–S(4)–C(5)	−82.7(4)
C(3)–S(4)–C(5)–C(6)	−177.4(3)
S(4)–C(5)–C(6)–S(7)	−66.2(4)
C(5)–C(6)–S(7)–C(8)	−91.5(4)
C(6)–S(7)–C(8)–C(9)	72.5(4)
S(7)–C(8)–C(9)–S(10)	53.2(5)
C(8)–C(9)–S(10)–C(11)	52.9(4)
C(9)–S(10)–C(11)–C(12)	65.9(4)
S(10)–C(11)–C(12)–S(1ⁱ)	74.0(5)
C(11)–C(12)–S(1ⁱ)–C(2ⁱ)	76.9(4)

Symmetry transformations used to generate equivalent atoms: i $-x + 1, -y + 1, -z + 1$; ii $-x + \frac{1}{2}, y, -z + 1$.

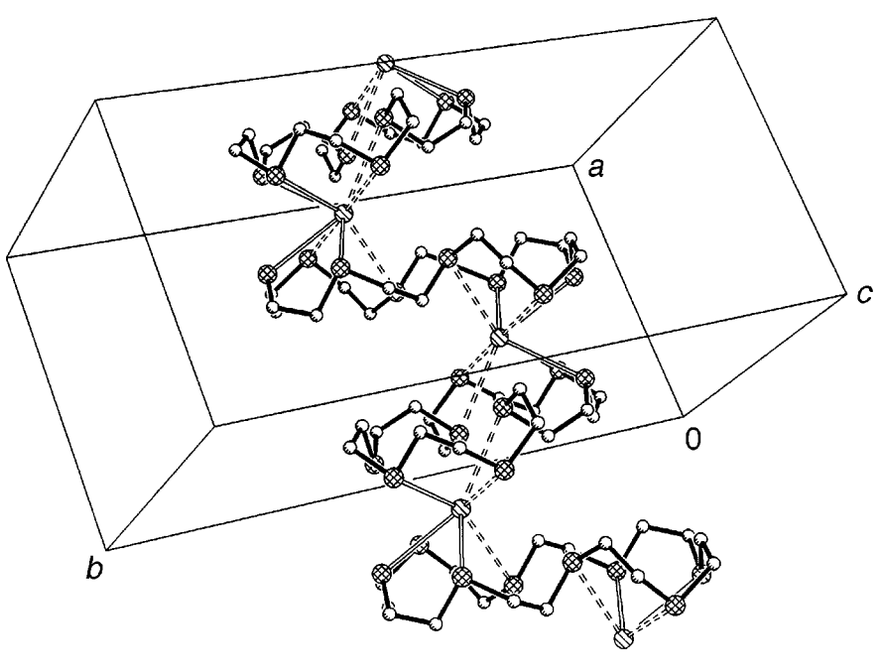

Fig. 7 Packing diagram for $[Tl([24]aneS_8)]PF_6$ showing the infinite one dimensional polymeric sequence along the *a* axis of thallium(I) ions and [24]aneS_8 molecules. The PF_6^- counter anions are not shown for clarity.

3.2851(13), Tl(1)–S(4) 3.2413(11) Å, lying within the sum of the formal ionic radii of S and Tl^{I} (1.84 + 1.59 = 3.43 Å)[38] suggesting a substantial covalency. The two other Tl–S distances are rather longer, Tl(1)–S(7) 3.4305(14), Tl(1)–S(10) 3.4734(14) Å, so they can be considered as short interactions. Apart from S(1)–Tl(1)–S(7), 116.29(3)°, all the S–Tl–S angles are quite acute (Table 4) ranging from 61.34(3) to 87.90(3)° consistent with the long Tl–S distances observed. We have observed similar Tl–S distances and acute S–Tl–S angles for the complexes $[Tl([9]aneS_3)]PF_6$[33] and $[Tl([18]aneS_6)]PF_6$[34] which represent the only previous examples of thioether macrocycle complexes of Tl^{I} reported. In $[Tl([9]aneS_3)]PF_6$ the trithia macrocycle is bound facially to the metal ion, Tl–S 3.114(3), 3.092(3), 3.110(3) Å, while a thioether donor from an adjacent cation makes a longer contact, Tl–S 3.431(3) Å, linking $[Tl([9]aneS_3)]^+$ cations into infinite helices. A similar situation is observed in $[Tl([18]aneS_6)]PF_6$ where all six macrocyclic S-donors interact with the metal centre at distances ranging from 3.164(5) to 3.356(6) Å and are disposed on one side of the Tl^{I}, with two much longer intermolecular interactions on the opposite side, Tl–S 3.689(6), 3.688(6) Å. The complex $[Tl([24]aneS_8)]PF_6$ represents the first example of a thioether macrocyclic complex of Tl^{I} having a genuine sandwich structure with half a ligand molecule bonded symmetrically on each side of the metal ion co-ordination sphere. Although in this structural situation Tl^{I} fulfils its stereochemical preference for relatively high co-ordination numbers, it is quite surprising to see this sandwich structure achieved with $[24]aneS_8$ for which the size mismatch between the Tl^{I} and the macrocyclic cavity should be reduced. A situation in which the metal ion is encapsulated within the ligand cavity might prevent a favourable geometric distribution of donor atoms about the Tl^{I} because of conformational constraints within the ligand.

Conclusions

The 24- and 28-membered octathia macrocyclic ligands have been used to synthesize complexes of p-block metal ions (Bi^{III}, Pb^{II}, Tl^{I}) and d^{10} transition metal ions (Ag^{I}, Hg^{II}, Cd^{II} and Au^{I}).[16] In all cases binuclear complexes have been isolated and structurally characterized and this demonstrates the ability of these ligands to bind two metal centres. In some cases polymeric complexes have also been obtained, expecially with the 24-membered ring, indicating that stereochemical and size mismatch with the complexed metal ion can also occur for these very large thioether macrocycles. The intramolecular metal–metal distances observed do not indicate any interaction, at least when the metal ions are in their stable electronic configurations. The possibility of these ligands stabilizing redox processes of metal centres through the formation of a metal–metal bond is now open to examination. The metals in which the d^8 and d^{10} configurations are stable (*e.g.* Pt, Pd and Au) would be of obvious interest. With Au we have already demonstrated that $[28]aneS_8$ is capable of supporting within its own co-ordination sphere a reversible four electron oxidation between the $Au^{I}Au^{I}$ and $Au^{III}Au^{III}$ species with the formation of transient Au^{II}-containing intermediates.[16b] The synthesis and electrochemical study of binuclear complexes of Pd^{II} and Pt^{II} with $[24]aneS_8$ and $[28]aneS_8$ is currently under investigation.

Experimental

Melting points are uncorrected. The IR spectra were recorded as KBr discs using a Perkin-Elmer 598 spectrometer over the range 200–4000 cm^{-1}. Microanalyses were performed by the University of Nottingham School of Chemistry Microanalytical Service. Mass spectra were recorded at the EPSRC National Mass Spectrometry Service at Swansea. **CAUTION:** the lead(II) complexes of $[24]aneS_8$ and $[28]aneS_8$ were isolated as ClO_4^- salts. We worked with these complexes on small scales both in solution and in the solid state without any incident. In spite of these observations, the unpredictable behaviour of ClO_4^- salts necessitates extreme care in their handling.

Preparations

$[(CdI_2)_2([24]aneS_8)]$. To a well stirred solution of $[24]aneS_8$ (20 mg, 0.0416 mmol) in MeCN–CH_2Cl_2 (15 cm^3 1:1 v/v) was added a solution of CdI_2 (30.76 mg, 0.084 mmol) in MeCN (5 cm^3). The mixture was stirred at room temperature for 2 h and the white solid formed filtered off, washed with CH_2Cl_2 and dried *in vacuo* (23.54 mg, 46.4% yield). Colourless block crystals suitable for X-ray diffraction studies were grown by allowing Et_2O to diffuse into a $MeNO_2$–thf solution (1:1 v/v) of the complex, mp 179–181 °C [Found (Calc. for $C_8H_{16}CdI_2S_4$): C, 16.15 (15.83); H, 2.70 (2.66)%]. FAB mass spectrum: *m/z* 720 (M^+); calc. for $[^{112}Cd([24]aneS_8)I]^+$ 720. IR spectrum (KBr disc): 2967w, 2911w, 1411s, 1289m, 1268m, 1250s, 1205s, 1144m, 911m, 856w, 827m, 722w and 700w cm^{-1}.

$[(BiCl_3)_2([24]aneS_8)]$. A mixture of $[24]aneS_8$ (25.64 mg, 0.0533 mmol) and $BiCl_3$ (33.61 mg, 0.1066 mmol) in MeCN (15 cm^3) was stirred at room temperature and under nitrogen atmosphere. A white microcrystalline powder was formed over 2 h. It was filtered off, washed with CH_2Cl_2 and dried *in vacuo* (43 mg, 72.6% yield). Crystals suitable for X-ray diffraction studies were grown by diffusion of Et_2O vapour into a solution of the complex in MeCN–thf (1:1 v/v), mp 152–153 °C; the white microcrystalline powder turns into an amorphous yellow wax, decomp. 183–185 °C [Found (Calc. for $C_8H_{16}BiCl_3S_4$): C, 17.59 (17.28); H, 2.94 (2.54)%]. IR spectrum (KBr disc): 2902w, 1601m, 1425s, 1247s, 1191w, 933m, 904m, 874w, 843m and 682w cm^{-1}. FAB mass spectrum, ES: very poor ionization, expected ions not found.

$[Pb_2([24]aneS_8)][ClO_4]_4$. A mixture of $[24]aneS_8$ (30 mg, 0.062 mmol) and $Pb(ClO_4)_2{\cdot}3H_2O$ (57.06 mg, 0.124 mmol) in CH_2Cl_2–MeCN (12 cm^3, 1:1 v/v) was stirred at room temperature for 4 h. The solvent was removed under reduced pressure and the white residue washed with CH_2Cl_2 and subsequently with Et_2O (15.1 mg, 21% yield). Colourless block crystals were grown by diffusion of Et_2O into a MeCN solution [Found (Calc. for $C_8H_{16}Cl_2O_8PbS_4$): C, 14.55 (14.86); H, 2.22 (2.48)%]. FAB mass spectrum: *m/z* 884, 787, 687; calc. for $[^{207}Pb([24]aneS_8)(ClO_4)_2]^+$, $[^{207}Pb([24]aneS_8)(ClO_4)]^+$ and $[^{207}Pb([24]aneS_8)]^+$ 887, 787 and 688 respectively. IR spectrum (KBr disc): 2978w, 2911w, 1422s, 1294w, 1250m, 1088 (br) s, 1035s, 917m, 894m, 839w, 817w and 622s cm^{-1}.

$[Pb_2([28]aneS_8)][ClO_4]_4$. A mixture of $[28]aneS_8$ (20 mg, 0.0372 mmol) and $Pb(ClO_4)_2{\cdot}3H_2O$ (34.24 mg, 0.0744 mmol) in MeCN–CH_2Cl_2 (15 cm^3, 1:1 v/v) was stirred at room temperature overnight. The white solid formed was filtered off and washed with CH_2Cl_2 (40.5 mg, 80.7% yield). Crystals suitable for X-ray diffraction studies were obtained by recrystallization from MeCN–Et_2O [Found (Calc. for $C_{10}H_{20}Cl_2O_8PbS_4$): C, 17.60 (17.79); H, 2.88 (2.96)%]. FAB mass spectrum: *m/z* 1249, 1150, 952; calc. for $[^{207}Pb_2([28]aneS_8)(ClO_4)_3]^+$, $[^{207}Pb_2([28]aneS_8)(ClO_4)_2]^+$ and $[^{207}Pb_2([28]aneS_8)]^+$ 1250, 1150 and 951.4 respectively. IR spectrum (KBr disc): 2950w, 2911w, 2844w, 1440m, 1412m, 1299w, 1274w, 1256m, 1139s, 1094s, 1033s, 922w, 905m, 767w and 622s cm^{-1}.

$[Tl([24]aneS_8)]PF_6$. To a solution of $[24]aneS_8$ (20 mg, 0.042 mmol) in CH_2Cl_2 (3 cm^3) was added a solution of $TlPF_6$ (14.52 mg, 0.042 mmol) in MeCN (3 cm^3). The resulting mixture was stirred at room temperature for 3 h. The solvent was partially removed under reduced pressure and a white solid precipitated

Table 5 Crystallographic data

Compound	$[(CdI_2)_2([24]aneS_8)]$	$[(BiCl_3)_2([24]aneS_8)]$	$[Pb_2([28]aneS_8)][ClO_4]_4$	$[Tl([24]aneS_8)]PF_6$
Formula	$C_{16}H_{32}Cd_2I_4S_8$	$C_{16}H_{32}Bi_2Cl_6S_8$	$C_{20}H_{40}Cl_4O_{16}Pb_2S_8$	$C_{16}H_{32}F_6PS_8Tl$
M	1213.3	1111.56	1349.18	830.24
Crystal system	Monoclinic	Triclinic	Monoclinic	Monoclinic
Space group	$P2_1/c$ (no. 14)	$P\bar{1}$ (no. 2)	$P2_1/n$ (no. 14)	$I2/a$ (no. 15)
a/Å	8.796(2)	8.644(2)	11.422(2)	10.868(2)
b/Å	8.037(2)	9.034(2)	14.806(3)	22.920(5)
c/Å	23.124(6)	11.269(3)	11.544(3)	11.269(2)
α/°		95.31(2)		
β/°	99.81(3)	100.89(2)	90.21(2)	93.84(3)
γ/°		112.38(2)		
U/Å^3	1610.8(2)	785.86(9)	1952.2(5)	2800.7(9)
Z	2	1	2	4
T/K	210(2)	150(2)	150(2)	203(2)
μ(Mo-Kα)/mm^{-1}	5.679	12.23	9.38	6.467
Reflections collected	2830	2781	3630	5343
Unique reflections, R_{int}	2830, —	2781, —	3469, 0.0509	2236, 0.0579
$R1$	0.0316 [2603 $F \geqslant 4\sigma(F)$]	0.0282 [2636 $F \geqslant 4\sigma(F)$]	0.0325 [3035 $F \geqslant 4\sigma(F)$]	0.0314 [2173 $F \geqslant 4\sigma(F)$]
$wR2$ (all data)	0.0798	0.0720	0.0741	0.0876

(unchanged $[24]aneS_8$). From the solution obtained after filtration, block crystals of the target compound were grown by Et_2O diffusion (14.3 mg, 41.42% yield). The same compound was obtained in 32% yield by performing the reaction with a $[24]aneS_8 : TlPF_6$ molar ratio of 1 : 2, mp 130–132 °C [Found (Calc. for $C_{16}H_{32}F_6PS_8Tl$): C, 22.95 (23.14); H, 3.70 (3.86)%]. FAB mass spectrum: m/z 685; calc. for $[^{205}Tl([24]aneS_8)]^+$ 685. IR spectrum (KBr pellet): 2922w, 1421m, 1262m, 1194w, 839s and 558m cm^{-1}.

Crystallography

A summary of the crystal data and refinement parameters for $[(CdI_2)_2([24]aneS_8)]$, $[(BiCl_3)_2([24]aneS_8)]$, $[Pb_2([28]aneS_8)][ClO_4]_4$ and $[Tl([24]aneS_8)]PF_6$ is given in Table 5. The crystals were cooled using an Oxford Cryosystems open-flow nitrogen cryostat.[44] For $[(CdI_2)_2([24]aneS_8)]$, $[(BiCl_3)_2([24]aneS_8)]$ and $[Pb_2([28]aneS_8)][ClO_4]_4$ data were collected on a Stoë STADI-4 four-circle diffractometer using ω–θ scans, whereas for $[Tl([24]aneS_8)]PF_6$ a Stoë IPDS image plate diffractometer was used. Data were corrected for Lorentz-polarization effects and absorption corrections (numerical or ψ scans) were also applied. The structures were solved by direct methods[45] and subsequent Fourier-difference syntheses.[46] All non-H atoms were refined anisotropically and all H atoms placed at calculated positions and thereafter refined using a riding model with $U_{iso}(H) = 1.2U_{eq}$ (C). For all the four structures the largest residual electron density features lay near the metal atoms. The structure of $[Pb_2([28]aneS_8)][ClO_4]_4$ shows disorder of the O(8) atom of the bridging perchlorate ions; the disorder was modelled by a partial occupancy model over two sites with occupancies of 0.57 and 0.43.

CCDC reference number 186/1154.

Acknowledgements

We thank the EPSRC, The University of Nottingham and the EPSRC National Mass Spectrometry Service at Swansea for support.

References

1 S. R. Cooper, *Acc. Chem. Res.*, 1988, **21**, 141; A. J. Blake and M. Schröder, *Adv. Inorg. Chem.*, 1990, **35**, 1; S. C. Rawle and S. R. Cooper, *Struct. Bonding* (*Berlin*), 1990, **72**, 1.
2 T. Adachi, M. D. Durrant, D. L. Hughes, C. J. Pickett, R. L. Richards, J. Talarmin and T. Yoshiba, *J. Chem. Soc.*, *Chem. Commun.*, 1992, 1464.
3 A. J. Blake, A. Taylor and M. Schröder, *Polyhedron*, 1990, **9**, 2911.
4 A. J. Blake, R. O. Gould, A. J. Holder, A. J. Lavery and M. Schröder, *Polyhedron*, 1990, **9**, 2919.
5 A. J. Blake, M. A. Halcrow and M. Schröder, *J. Chem. Soc.*, *Dalton Trans.*, 1994, 1631 and refs. therein.
6 C. Landgrafe and W. S. Sheldrick, *J. Chem. Soc.*, *Dalton Trans.*, 1996, 989.
7 K. Brandt and W. S. Sheldrick, *J. Chem. Soc.*, *Dalton Trans.*, 1996, 1237.
8 A. J. Blake, D. W. Bruce, I. A. Fallis, S. Parsons, H. Richtzenhain, S. A. Ross and M. Schröder, *Philos. Trans. R. Soc. London*, *Ser. A*, 1996, **354**, 395.
9 R. D. Adams, S. B. Fallon, J. L. Perrin, J. A. Queisser and J. H. Yamamoto, *Chem. Ber.*, 1996, **129**, 313 and refs. therein.
10 G. J. Grant, K. E. Rogers, W. N. Setzer and D. G. Van Derveer, *Inorg. Chim. Acta*, 1995, **234**, 35.
11 H.-J. Kim, J.-H. Lee, I.-H. Suh and Y. Do, *Inorg. Chem.*, 1995, **34**, 796.
12 M. Munakata, L. P. Wu, M. Yamamoto, T. Kuroda-Sowa and M. Maekawa, *J. Chem. Soc.*, *Dalton Trans.*, 1995, 3215.
13 A. J. Blake, A. J. Holder, T. J. Hyde and M. Schröder, *J. Chem. Soc.*, *Chem. Commun.*, 1987, 987; A. J. Blake, R. O. Gould, A. J. Holder, T. I. Hyde, A. J. Lavery, M. O. Odulate and M. Schröder, *J. Chem. Soc.*, *Chem. Commun.*, 1987, 118; S. C. Rawle, R. Yagbasan and S. R. Cooper, *J. Am. Chem. Soc.*, 1987, **109**, 6181.
14 A. J. Blake, R. O. Gould, A. J. Holder, T. I. Hyde and M. Schröder, *J. Chem. Soc.*, *Dalton Trans.*, 1988, 1861; A. J. Blake, R. O. Gould, J. A. Greig, A. J. Holder, T. I. Hyde and M. Schröder, *J. Chem. Soc.*, *Chem. Commun.*, 1989, 876; A. J. Blake, R. O. Gould, J. A. Greig, A. J. Holder, T. I. Hyde, A. Taylor and M. Schröder, *Angew. Chem.*, *Int. Ed. Engl.*, 1990, **29**, 197.
15 (*a*) A. J. Blake, A. J. Holder, T. I. Hyde, G. Reid and M. Schröder, *Polyhedron*, 1989, **8**, 2041; (*b*) W. N. Setzer, Q. Guo, G. J. Grant, J. L. Hubbard, R. L. Glass and D. G. VanDerveer, *Heteroatom Chem.*, 1990, **1**, 317; (*c*) T. E. Jones, L. S. W. L. Sokol, D. B. Rorabacher and M. D. Glick, *J. Chem. Soc.*, *Chem. Commun.*, 1979, 140.
16 (*a*) A. J. Blake, W.-S. Li, V. Lippolis and M. Schröder, *Chem. Commun.*, 1997, 1943; (*b*) A. J. Blake, W.-S. Li, V. Lippolis, A. Taylor and M. Schröder, *J. Chem. Soc.*, *Dalton Trans.*, 1998, 2931.
17 R. E. DeSimone and T. M. Tighe, *J. Inorg. Nucl. Chem.*, 1976, **38**, 1623; K. Travis and D. H. Bush, *Chem. Commun.*, 1970, 1041; A. C. Braithwaite, C. E. F. Richard and T. N. Waters, *Aust. J. Chem.*, 1981, **34**, 2665; K. Saito, Y. Masudo and E. Sekido, *Anal. Chim. Acta*, 1983, **151**, 447; D. Sedvic and H. Meider, *J. Inorg. Nucl. Chem.*, 1977, **39**, 1403.
18 N. Alcock, N. Herron and P. Moore, *J. Chem. Soc.*, *Dalton Trans.*, 1978, 394.
19 A. J. Blake, E. C. Pasteur, G. Reid and M. Schröder, *Polyhedron*, 1991, **10**, 1545.
20 (*a*) W. N. Setzer, Y. Tang, G. J. Grant and D. G. VanDerveer, *Inorg. Chem.*, 1991, **30,** 3652; (*b*) R. S. Glass, L. K. Steffen, D. D. Swanson, G. S. Wilson, R. deGelder, R. A. G. deGraaff and J. Reedijk, *Inorg. Chim. Acta*, 1993, **207**, 241; (*c*) J. Pickardt and J. Shenn, *Z. Naturforsch.*, *Teil B*, 1993, **48**, 969.
21 W. N. Setzer, Y. Tang, G. J. Grant and D. G. VanDerveer, *Inorg. Chem.*, 1992, **31**, 1116.
22 A. J. Blake, R. O. Gould, G. Reid and M. Schröder, *J. Chem. Soc.*, *Chem. Commun.*, 1990, 974.
23 B. De Groot and S. J. Loeb, *Inorg. Chem.*, 1991, **30**, 3103.
24 A. J. Blake, R. O. Gould, A. J. Holder, T. I. Hyde and M. Schröder, *Polyhedron*, 1989, **8**, 513.

25 H. J. Küppers, K. Wieghardt, Y. H. Tsay, C. Krüger, B. Nuber and J. Weiss, *Angew. Chem.*, *Int. Ed. Engl.*, 1987, **26**, 575.
26 J. Clarkson, R. Yagbasan, P. J. Blower, S. C. Rawle and S. R. Cooper, *J. Chem. Soc.*, *Chem. Commun.*, 1987, 950.
27 P. J. Blower, J. A. Clarkson, S. C. Rawle, J. R. Hartman, R. E. Wolf, jun., R. Yagbsan, S. G. Bott and S. R. Cooper, *Inorg. Chem.*, 1989, **28**, 4040.
28 A. J. Blake, D. Collison, R. O. Gould, G. Reid and M. Schröder, *J. Chem. Soc.*, *Dalton Trans.*, 1993, 521.
29 R. Alberto, W. Nef, A. Smith, T. A. Kaden, M. Neuburger, M. Zehnder, A. Frey, U. Abram and P. A. Schubiger, *Inorg. Chem.*, 1996, **35**, 3420.
30 H.-J. Küppers, K. Wieghardt, B. Nuber and J. Weiss, *Z. Anorg. Allg. Chem.*, 1989, **577**, 155.
31 G. H. Robinson and S. A. Sangokoya, *J. Am. Chem. Soc.*, 1988, **110**, 1494.
32 G. H. Robinson, H. Zhang and J. L. Atwood, *Organometallics*, 1987, **6**, 887.
33 A. J. Blake, J. A. Greig and M. Schröder, *J. Chem. Soc.*, *Dalton Trans.*, 1991, 529.
34 A. J. Blake, G. Reid and M. Schröder, *J. Chem. Soc.*, *Dalton Trans.*, 1992, 2987.
35 G. R. Willey, M. T. Lakin and N. W. Alcock, *J. Chem. Soc.*, *Dalton Trans.*, 1992, 591.
36 G. R. Willey, M. T. Lakin, M. Ravindran and N. W. Alcock, *J. Chem. Soc.*, *Chem. Commun.*, 1991, 271.
37 G. R. Willey, A. Jarvis, J. Palin and W. Errington, *J. Chem. Soc.*, *Dalton Trans.*, 1994, 255.
38 R. D. Shannon, *Acta Crystallogr.*, *Sect. A*, 1976, **32**, 751.
39 S. C. Nyburg, G. A. Ozin and J. T. Szymanski, *Acta Crystallogr.*, *Sect. B*, 1971, **27**, 2298.
40 M. G. B. Drew, D. G. Nicholson, I. Sylte and A. Vasudevan, *Inorg. Chim. Acta*, 1990, **171**, 11.
41 M. M. Olmstead, R. M. Kessler, H. Hope, M. D. Yanuck and W. K. Musker, *Acta Crystallogr.*, *Sect. C*, 1987, **43**, 1890.
42 (*a*) E. C. Constable, C. Sacht, G. Palo, D. A. Tocher and M. R. Truter, *J. Chem. Soc.*, *Dalton Trans.*, 1993, 1307; (*b*) A. Bashall, M. McPartlin, B. P. Murphy, H. R. Powell and S. Waikar, *J. Chem. Soc.*, *Dalton Trans.*, 1994, 1383; (*c*) K. R. Adam, D. S. Baldwin, A. Bashall, L. F. Lindoy, M. McPartlin and H. R. Powell, *J. Chem. Soc.*, *Dalton Trans.*, 1994, 237; (*d*) P. Hoffmann, F.-J. Hermes and R. Mattes, *Z. Naturforsch.*, *Teil B*, 1988, **43**, 567.
43 L. S. Livny, J. P. Glusker and C. W. Bock, *Inorg. Chem.*, 1998, **37**, 1853.
44 J. Cosier and A. M. Glazer, *J. Appl. Crystallogr.*, 1986, **19**, 105.
45 G. M. Sheldrick, SHELXS 86, SHELXS 97, Programs for Crystal Structure Solution, University of Göttingen, 1986, 1997.
46 G. M. Sheldrick, SHELXL 93, SHELXL 97, Programs for Crystal Structure Refinement, University of Göttingen, 1993, 1997.

Paper 8/05137B